Fast Particle Physics on ASDEX Upgrade – Interaction of Energetic Particles with Large and Small Scale Instabilities

S. Günter[1], G. Conway[1], H.-U. Fahrbach[1],C. Forest[2], M. Garcia Muñoz[1], S. daGraca[3], T. Hauff[1], J. Hobirk[1],V. Igochine[1], F. Jenko[1], K. Lackner[1], P. Lauber[1], P. McCarthy[4], M. Maraschek[1], P. Martin[5], E. Poli[1], K. Sassenberg[4], E. Strumberger[1], G. Tardini[1], H. Zohm[1], ASDEX Upgrade Team
[1] Max-Planck Institut für Plasmaphysik, Garching, Germany, EURATOM Association
[2] Dept. of Physics, University of Wisconsin, Madison, Wisconsin, USA
[3] Centro de Fusão Nuclear, Associa cão EURATOM/IST, Instituto Superior Técnico, Lisboa, Portugal
[4] Physics Department, University College Cork, Cork, Ireland
[5] Consorzio RFX, Assozione EURATOM-ENEA per la fusione, Padova, Italy

e-mail contact of main author: Sibylle.Guenter@ipp.mpg.de

Abstract. Beyond a certain heating power, measured and predicted distributions of NBI driven currents deviate from each other, in a form that can be explained by the assumption of a modest diffusion of fast particles. Direct numerical simulation of fast test particles in a given field of electrostatic turbulence indicates that for reasonable parameters fast and thermal particle diffusion indeed are similar. - High quality plasma edge plasma profiles on ASDEX Upgrade, used in the linear, gyrokinetic, global stability code LIGKA give excellent agreement with the eigenfunction measured by a newly extended reflectometry system for ICRH-excited TAE-modes. They support the hypothesis of TAE-frequency crossing of the continuum in the edge region as explanation of the high TAE-damping rates measured on JET.- A new fast ion loss detector with 1MHz time resolution allows frequency and phase resolved correlation between low frequency magnetic perturbation, giving, together with modelling of the particle orbits, new insights into the mechanism of fast particle losses during NBI and ICRH due to helical perturbations.

1. Introduction

It is well recognized that the interaction of fast particles with large scale magnetic perturbations can have a major influence on heating efficiencies and wall loading. Recently, discrepancies have been found between the predicted and observed current profile modifications due to off-axis NBI, correlated with the increase of heating power and of turbulent energy losses [1,2]. It has therefore been surmised that small scale turbulence, driven by gradients in the thermal plasma profiles, might also act on suprathermal particles. ASDEX Upgrade is well equipped for such studies, due to its powerful and flexible heating system (up to 20 MW NBI at 60/93 keV; up to 6MW ICRH, up to 2 MW ECRH) and its well developed diagnostics. Recent relevant additions to the latter consist in a high-time resolution fast ion loss detector [3], and upgrades to the reflectometry system. In parallel we have been developing the theoretical tools for the study of instabilities driven by fast particles (in the form of a linear global gyrokinetic stability code, which includes a full description of the fast particle orbits) and of the effect of background plasma turbulence on fast particle dynamics.

2. Current Profile Modification by off-axis NBI on ASDEX Upgrade

ASDEX Upgrade is equipped with a flexible NBI heating system, allowing on- and off-axis heating and current drive. In a typical scenario for NBI current-redistribution experiments we pass through a sequence: on-axis/off-axis/on-axis beam injection, with the length of the phases chosen to allow approach to resistive equilibrium. The off-axis injection is complemented by central ECRH, adjusted in power to keep the electron temperature, and

hence the resistivity, approximately constant in time [2,4]. All experiments reported in the following were in type-I ELMy H-mode regime. The two off-axis beam-sources, with a beam voltage of 93keV and a total power of up to 5 MW have a tangency radius of 1.29 m (nominal major radius of ASDEX Upgrade: 1.65m) and are inclined vertically to be tangent, in a poloidal cut, to the half-minor radius flux surface. The on-axis beam sources (total power up to 15 MW) operate at 60 keV (4 sources) and 93keV (2 sources) respectively. The MSE system is linked to operation of one of the more radially directed 60 keV sources (tangency radius 0.93m).

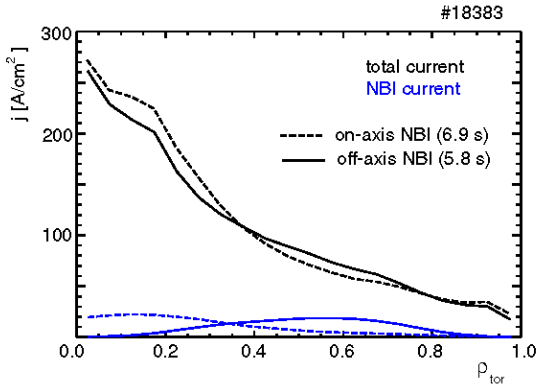

Fig. 1: TRANSP results for NBI (blue) and total (black) current density profiles at the end of the off-axis (solid) and the on-axis phase (dashed).

At sufficiently low total heating power the measured time traces of the MSE signal correspond very well to the TRANSP prediction [2]. At high triangularity (δ~0.4), this regime extends up to our full off-axis power capability. Fig. 1 shows the modelled NBI and total current densities for two time instances, at the end of the off-axis and the second on-axis phase. Such changes in the current density profiles for low power discharges are also confirmed by the observed shift in the resonance location of occasionally appearing MHD activity. In the high heating power regime (which for low triangularity (δ~0.2) is reached with less than 5 MW) the current profile changes measured by the MSE system fall significantly short of the predictions of the TRANSP code. The agreement can be substantially improved by introducing an artificial diffusion of the slowing down fast particles, assuming a diffusivity $D_{fast} \approx 0.5 m^2/s$. Fig. 2 shows the TRANSP current density profiles at the end of the off-axis and on-axis injection phases, computed both with and without fast particle diffusion. The consequences of fast particle diffusion on the NBI-driven current density distribution are illustrated in Fig. 3 for the off-axis case.

The predicted total driven current, as monitored by the loop voltage, agrees quite well with TRANSP simulations throughout all power regimes, even without the assumption of additional fast particle diffusion. The latter is, anyway, expected to affect the net-current drive efficiency only through higher order effects (e.g. by displacing particles into regions with different slowing-down rate). Nevertheless, simulations with fast particle diffusion appear to give also in this respect a slightly better fit [2].

More direct information of the radial distribution of the NBI driven currents and their temporal behaviour can be found from the radial profiles of the parallel electric field. The latter follow from equilibrium reconstructions, using time dependent measurements of MSE angles and loop voltage [5,6]. For the loop voltage profiles shown in Fig. 4, the procedure described in [7,8] has been applied, using equilibrium reconstruction procedures in the CLISTE code [9,10]. Immediately after switching from on-axis to off-axis beams (and back), the profiles show the expected behaviour: the loop voltage decreases at the radial location of the respective beam deposition. Within a time much shorter than the current redistribution time however, the loop voltage flattens again. As no strong MHD activity is present in the

discharge (except for small fishbones in the very plasma centre), current redistribution cannot have been completed within this time. Within this time only the source of the current, the fast particles, can be redistributed.

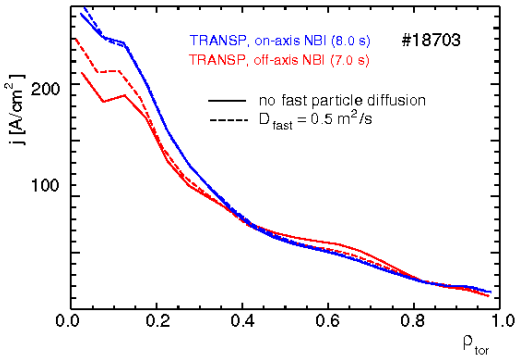

Fig. 2: TRANSP current density profiles at the end of the off-axis (red) and the on-axis phase (blue) for a "high heating power" discharge, with (dashed) and without (solid) fast particle diffusion.

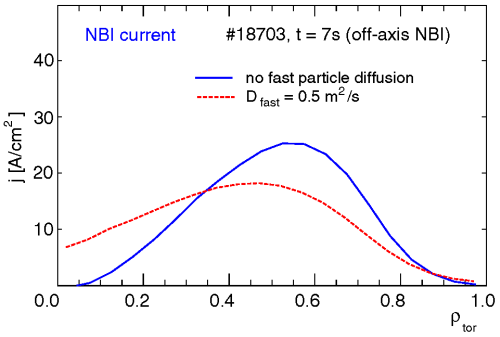

Fig. 3: TRANSP results for NBI current density profiles for off-axis NBI, without (blue) and with (red) artificially introduced fast particle diffusion.

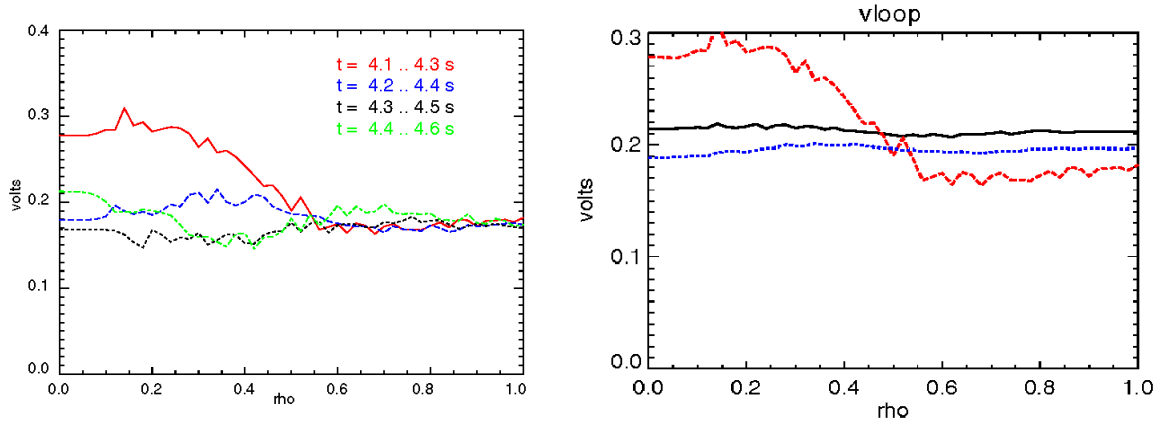

Fig. 4:Left: Time sequence of radial loop voltage profiles for the ASDEX Upgrade discharge #19174 (averaged over 200 ms) after switching from on- to off-axis beams at 4.1 s. Right: Stationary loop voltage profile for the on-axis beam phase (black), the beginning of the off-axis phase (red) and the stationary loop voltage profile for the off-axis beam phase (blue) The difference in the stationary loop voltages demonstrates the larger current drive capability by the off axis beam. The total heating power is 5 MW in a low triangularity discharge, the off-axis beams are reduced in voltage to restrict the fast ion velocity below $v_A/3$.

Obvious candidate mechanisms for a fast-particle re-distribution are Alfvén-type waves or other MHD activity. To rule out m/n = 1/1 type MHD activity of fishbone or sawtooth type we have carried out the NBI current re-distribution experiments also at higher q_{95} values corresponding to vanishing (1/1) activity, with similar results for the observed and modelled NBI current distribution. To rule out a possible role of Alfvén waves, we have also carried out experiments varying the resonance conditions for such waves, e.g. by reducing the beam velocity below $v_A/3$, without change in the observed behaviour. We also have found no direct evidence for Alfvén wave activity, in spite of a dedicated search with Mirnov, SXR and

reflectometry diagnostics. It should also be noted that observations of Alfvén activity for $v_{\|} < v_A/3$ in other experiments appear to be restricted so far to hollow-q profiles (see e.g. [11]), a situation not pertinent to our experiments.

3. Turbulent ExB advection of fast test particles

The result described above, and in particular the apparent correlation with the thermal heat transport has raised interest in the more general question of the response of suprathermal particles to background plasma turbulence. It has been argued that the interaction of fast ions with the background turbulence should be small - mainly because of their large gyroradius which gyro-averages out electrostatic potential fluctuations. However, the recent de-correlation trajectory theory put forward by M. Vlad et al. [12] has shown this picture to be oversimplified, as gyro-averaging also leads to a broadening of the zone of influence of an individual eddy. For a more direct assessment we have carried out direct numerical simulation of an assembly of test particles in a constant background magnetic field and a prescribed turbulent spectrum of electrostatic fluctuations, using either a full-orbit, or a gyrokinetically averaged model of particle motion (with no difference in the results between the two models). The problem is defined by two characteristic parameters: the Kubo number, suitably defined for this case by $K = V_{E\times B}\tau_c/\lambda_c$ (v_{ExB}: ExB velocity, τ_c, λ_c: correlation time and length of the turbulent potential), and ρ/λ_c (ρ being the gyroradius of the test particles). Core turbulence is typically found to peak around $2\pi/k_y\rho_s \approx 20-30$, corresponding to $\rho/\lambda_c \approx 1$ for thermonuclear α-particles and correspondingly smaller values for our beam ions. The results of our test

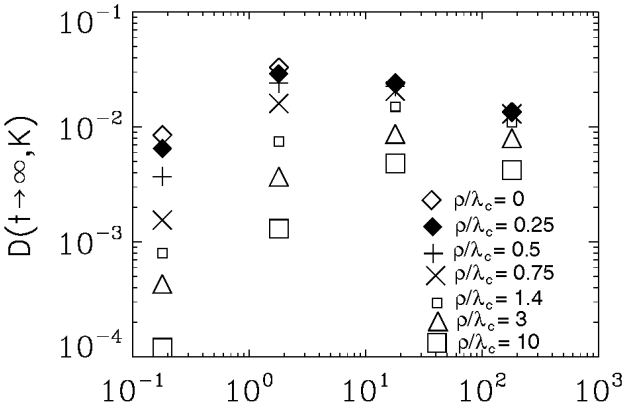

Fig. 5 Long-time limit of the diffusivity D as a function of the Kubo number K for different gyroradii ρ, normalized to the correlation length of the potential λ_c

particle simulations, illustrated in Fig. 5, show a very large reduction of turbulent diffusion by finite gyro-radius effects for relevant ρ/λ_c - values only at small Kubo numbers. Based on simulations with the nonlinear gyrokinetic code GENE we expect the Kubo numbers under realistic experimental conditions to be of the order of unity or even larger. In this range the diffusion coefficient for fast particles is not significantly different from that of cold test-particles. That way, one finds that for Kubo numbers up to about unity, the test particle transport drops quickly with increasing gyroradius, but for larger Kubo numbers (typical for strong plasma turbulence), the dependence on the gyroradius is relatively weak (as long as it is smaller than a few perpendicular correlation lengths of the turbulence). These numerical results can be also understood in terms of a modified form of decorrelation trajectory theory [13]. Regarding our experimental findings, these results support our interpretation in terms of a correlation between increased thermal transport and enhanced fast particle diffusion leading to a broadening of the distribution of NBI driven currents.

4. Damping of TAE modes

The nature and magnitude of the dominating TAE damping mechanism are decisive for the amplitude of fast-particle excited TAE modes and hence for the associated particle and energy losses. Direct measurements of damping rates of externally excited TAE modes on JET showed large values, explained at that time by a gyrokinetic model as being due to radiative damping in the plasma centre [14]. Other gyrokinetic codes, developed in the meantime, and analytic models, however did not confirm this explanation [15, 16]. An alternative explanation presupposes the intersection of the TAE frequency and the continuum Alfvén spectrum at the plasma edge. This possibility depends sensitively on edge profiles and could not be ruled out within the experimental uncertainties of the density measurements. To examine quantitatively this and other aspects of the damping and excitation of Alfvén waves we have developed a linear, fully gyrokinetic, non-perturbative eigenvalue code, including realistic fast particle orbits: LIGKA [16]. It has been extensively benchmarked against other codes in their respective range of validity. With this code, indeed, satisfactory quantitative agreement with the measured damping rates could be achieved under assumptions leading to closed gaps in the Alfvén spectrum. Conclusive experiment-theory comparisons require, however, accurate measurements of both the density profiles and of the eigenfunction of the excited modes. The former are available with high quality for ASDEX Upgrade using a combination of Thomson scattering, Lithium beam and reflectometry data. Eigenfunction measurements in the core with SXR can now be complemented by reflectometry measurements in the edge region. In a frequency hopping mode the latter are used – under conditions of stationary TAE activity – to probe the density fluctuations at different radial locations, using correlation techniques to reconstruct the envelope of the TAE eigenfunction

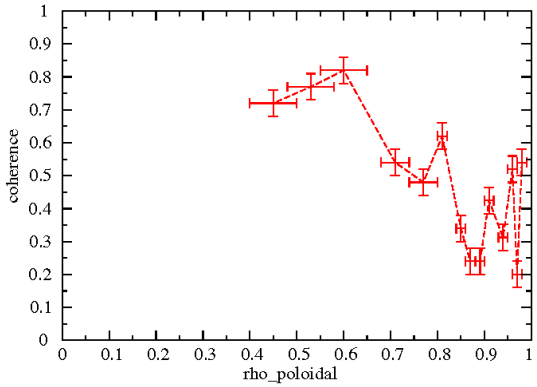

Fig. 6a: Radial coherence profile of reflectometry and magnetic measurements for a n=4 TAE mode

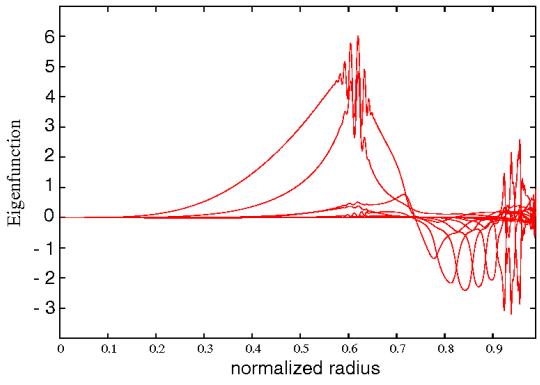

Fig. 6b: LIGKA-Eigenfunction for the n=4 TAE mode

[17,18]. Fig. 6a and 6b are experimental and LIGKA results for an n = 4 TAE perturbation excited by ICRH heating of a low density discharge, where the peaked density profile allows for reflectometry measurements up to the plasma core. As experimental data we show the coherence between magnetic and reflectometry signals. Measured density profiles and reconstructed plasma equilibria lead to closed TAE gaps in this case, as is usual for ASDEX Upgrade H-mode discharges. The observed TAE frequencies and the location of their maximum amplitude in the SXR signals, were used together with MSE measurements as constraints in the q-profile reconstruction. The gyrokinetic results of LIGKA for this case show a good agreement with the experiment (note that no phase information is involved in the

experimental data, i.e. they correspond to the absolute value of the amplitude of the perturbation). In particular they reproduce well the rapid oscillations of the eigenfunction, as being caused by finite Larmor-radius effects in the region of the crossing of the gap (beyond a normalized radius of 0.9), and as a direct indication for a closed gap. In fact, only for such closed gaps do gyrokinetic codes give damping rates for the least damped modes in the range observed on JET.

5. Interaction of fast particles with magnetic perturbations

New insights into the interaction between fast particles and large scale magnetic perturbations have been gained by the deployment of a fast ion loss detector [3] following the principle design used on TFTR and later W7-AS. In addition to the observation with a CCD camera an array of photomultipliers, with a bandwidth of 1 MHz is used. The high time resolution of the latter allows not only frequency but also phase correlation of particle losses with MHD fluctuations, and such correlations have in fact been clearly observed not only for TAEs, but also for lower frequency magnetic perturbations (NTMs, double tearing modes, ELMs). In case of NBI produced particles the capability of intermittent operation of the sources, with a switch--off time of less than 50 μs, gives additional information on the origin of the observed fast particles. MHD perturbations leading to large islands give origin to losses to the detector,

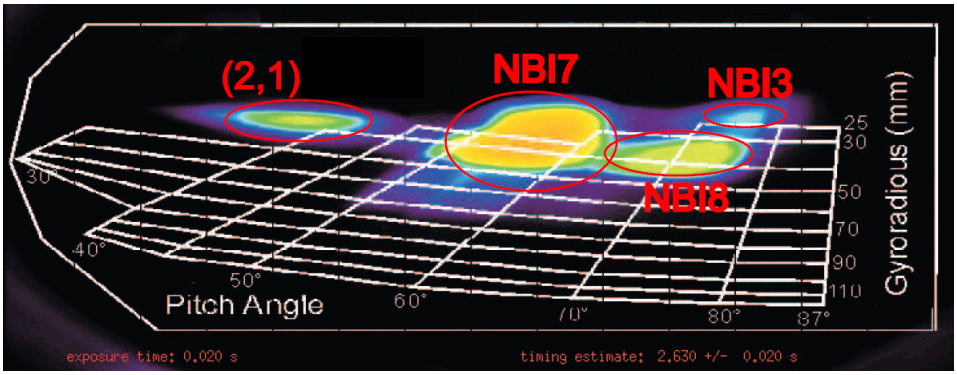

Fig. 7: CCD view of the light pattern produced by ion impacts on the scintillator plate for ASDEX Upgrade #21168.

which are modulated with the mode frequency and phase locked with it. In these cases the phase velocity of the mode is much smaller than the fast particle velocity. Fig. 7 shows a CCD camera picture of the detector during a double-tearing event, for standard, co-directed beam orientation. The luminous patches can be assigned to fixed pitch-angle and energy windows. The three most prominent correspond (from the left) to high field side deposition of the more radial 93 keV source (source #8), low field side deposited particles of the more tangential source (source #7) and low field side deposition of #8. All three show a strong modulation with the amplitude closely related to that of the magnetic perturbation [19]. Switch-on/-off experiments of source #8 show an immediate (within 5-15 μs) total decay of the signal, demonstrating that particles are lost within the first 2-3 toroidal orbits. This is in agreement with the fact that these particles are deposited on the high-field side well inside the separatrix, and can cross it readily on the low-field side due to the torus drift displacement of their orbits. The modulation with the island frequency can be explained by the formation of drift islands with (3,1) and (4,1) helicities. Low-field side deposited particles, if ionized outside the separatrix, can reach immediately and without any magnetic perturbation the

detector), and are observed to respond immediately to the switch-off of the NBI source (Fig. 8, left). Co-directed particles deposited inside the separatrix on the low field side, on the other hand, can reach the detector only after being displaced to outer flux surfaces. In fact, low field side deposited particles of source #8 respond with a much larger delay (of the order of 5 ms) to the switching-off of the source (Fig. 8, right). From the source geometry, the pitch-angle and energy window of the detector, and the fact that in the corresponding energy and

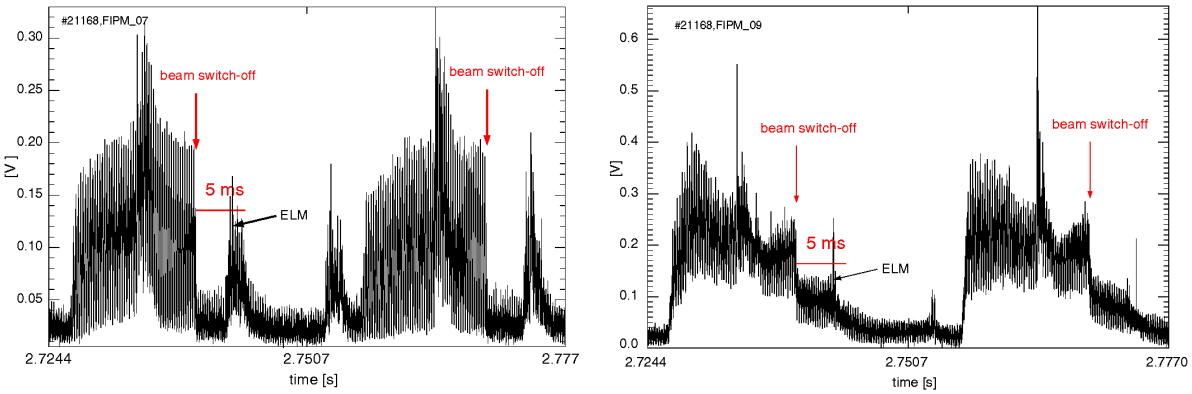

Fig. 8: Response of the fast ion losses to switch-on and –off of the NBI source #8. Left for particles deposited on the high field side, right for particles deposited on the low field side.

temperature range pitch angle scattering is not important, the radial range over which the observed ions are first deposited in the plasma can be estimated to extend to about 10 cm inside the separatrix. According to drift orbit calculations using the Orbit and the Gourdon code, this time-decay of the signal can be explained to be due to a region of orbit stochasticity [16], leading to drift orbit losses proceeding over many (order > 10^2) toroidal particle transits, and limited in time probably by the collisional slowing down of the fast particle population (which, in the edge region, would also correspond to a few ms). Source #7, also giving a signal from its low-field side deposited particles on Fig.7, was not run in an intermittent mode. The decay of its signal after switching-off shows, however, again a slow (ms time-scale) as well, similar to the low-field side deposited particles of source #8. On the other hand FILD (fast-ion-loss-detector) signals during the switch-off phase of experiments at lower heating power, without large MHD activity, show an immediate decay of the observed losses following source switch-off. The observed strong increase of fast ion losses caused by magnetic islands is consistent with the observation of increased heat loads to the limiters found in experiments as soon as large magnetic islands appear.

Frequency and phase related modulation of losses were also observed for more energetic, ICRH produced particles, in a pitch-angle range corresponding to strong trapping. Calculations with the HAGIS code [21] yield a possible explanation in terms of a resonance of the bouncing particle orbits with a (3,2) NTM (Fig. 9). For particles of certain pitch angle and energy (within the experimentally expected range) bounce orbits return nearly to the same poloidal and toroidal location – and hence to a fixed phase of the magnetic perturbation, assuming the latter for the moment as stationary - after an integer number n of bounces. This implies that the (radial) motion induced by the perturbed field lines, which usually averages to zero over a few bounce times, can lead to a net radial drift of the trapped-particle orbits, inwards or outwards depending on the phase of the orbit with respect to the island [22]. This resonance condition can be satisfied also in the presence of a non-vanishing $v_{prec} - 2\pi R/(n\tau_{bounce})$, which has to be equal to the toroidal phase velocity of the mode.

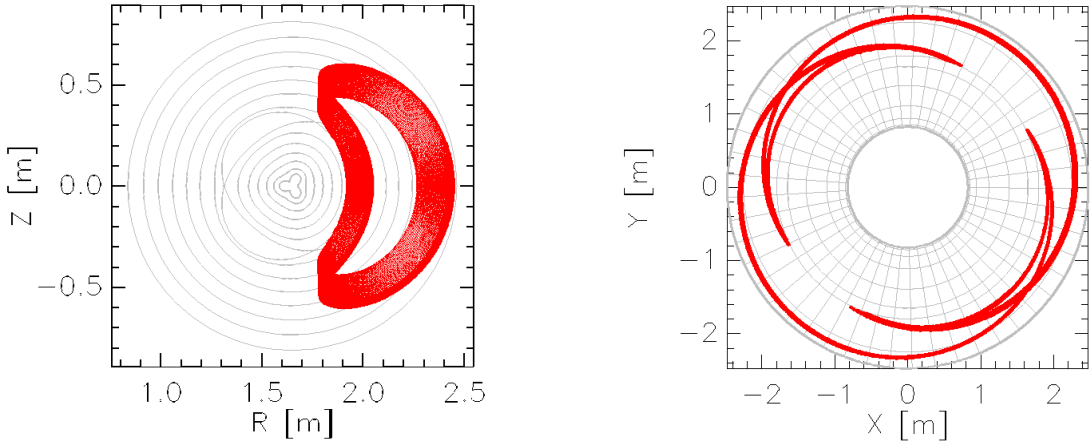

Fig. 9: Radial drift of an ICRH produced particle (energy: 600 keV) according to HAGIS calculations due to an n=2 magnetic island (left). The particle orbit shows an n=2 symmetry, allowing for a constant phase relation between particle and magnetic island.

References

[1] J. Hobirk et al. 30th EPS conference, St. Petersburg, Russia, 2003, O-4.1B
[2] S. Günter et al., 31st EPS conference, London, UK, 2004, O1.02, 32st EPS conference, Tarragona, Spain, 2005, P-4.075
[3] M. Garcia Muñoz et al., 32st EPS conference, Tarragona, Spain, 2005, P-5.085
[4] S. Günter et al., Nucl. Fusion **45**, S98, 2005
[5] C.B. Forest et al., Phys. Rev. Lett **73**, 2444 (1994)
[6] J.K. Anderson et al., Phys. Plasmas **11**, L9 (2004)
[7] C.B. Forest et al., 33st EPS conference, Rome, Italy, 2006, P2.129
[8] P.J. McCarthy et al., 33st EPS conference, Rome, Italy, 2006, P2.144
[9] K. Lackner, Comp. Phys. Comm. **12**, 33 (1975)
[10] P.J. McCarthy, Phys. Plasmas **6**, 2834 (1999)
[11] R. Nazikian et al., 20th IAEA FEC, Vilamoura, Portugal, 2004, IAEA-CN-116/EX/5-1
[12] M. Vlad and F. Spineanu, Plasma Phys. Control. Fusion **47**, 281 (2005)
[13] T. Hauff and F. Jenko, in print, Phys. Plasmas (2006)
[14] A. Fasoli, A. Jaun, and D. Testa, Phys. Lett. **A 265**, 288 (2000)
[15] G. Y. Fu, H.L. Berk, and A. Pletzer, Phys. Plasmas **12**, 082505 (2005)
[16] H.E. Mynick, Phys. Fluids B5, 1471 (1993)
[17] Ph. Lauber, S. Günter, S. Pinches, Phys. Plasmas **12**, 122501 (2005)
[18] L. Cupido et al., Rev. Sci. Instrum. **75**, 3865 (2004)
[19] S. Da Graca et al., 33th EPS conference, Rome, 2006, P2.146
[20] M. Garcia Muñoz et al., to be published
[21] S. D. Pinches et al., Comp. Phys. Comm. **111**, 131 (1998)
[22] E. Poli, to be published